



Preparation mechanism for neodymium doped strontium phosphate and its spectroscopic, optical and electrical characteristics

Bindu Raina, Seema Verma, Goldy Slathia, Rashmi Gupta, K.K. Bamzai*

**Crystal Growth & Material Research (CGMR) Lab, Department of Physics,
University of Jammu, Jammu-180006 (India)**

Abstract : The growth of neodymium doped strontium phosphates (NdSrP) materials involves the system $\text{Nd}(\text{NO}_3) - \text{SrCl}_2 - \text{H}_3\text{PO}_4 - \text{Na}_2\text{SiO}_3$. The optimum conditions involved for the growth of NdSrP were found out. These are found to be highly efficient laser crystals with good electro-optic and conducting properties. X-ray diffraction (XRD), particle size analyzer, scanning electron microscopy (SEM), ultraviolet spectroscopy (UV), Fourier transform infrared spectroscopy (FTIR), and dielectric studies were performed to characterize the samples. The material belongs to triclinic crystal system with well defined and highly resolved crystalline peaks. The electron micrograph clearly depicts the spherulitic morphology that has further grown in the form of elongated plates. The presence of various atomic bonds within a molecule and the functional groups along with the relevant P - O bonds were found by Fourier transform infrared (FTIR) method. Ultraviolet (UV) spectroscopy is an important technique to explore the optical properties of a given material viz., electronic transitions and optical band gap. The optical transmittance range and transparency cut off depict that material possess enhanced optical characteristics. The electric analysis establishes the material to be normal dielectric and the dielectric constant is strongly temperature and frequency dependent.

Keywords : Electrical properties, doping, electro-optic, dielectric constant, phosphates.

1. Introduction

The technology and science of materials has flourished and advanced in a very brisk manner and phosphates technically form the strong backbone to these materials. Phosphates represent the most interesting class of materials and are considered to be technically very promising materials. The room temperature solution growth technique appeared quiet attractive for growing crystals of group II compounds on account of its unique advantages in terms of crystal produced and the simplicity of process [1-3]. The alkaline earth phosphates have assumed greater importance in view of their use as phosphor matrices [4]. Neodymium doped crystals have found a wide variety of application in military, industry, medical treatment and scientific research. So, the emphasis was given on the growth of neodymium doped strontium phosphates because of the combination of rare earth element with the phosphate group. Kanchana et al [5] carried out the growth of strontium chromium

K.K. Bamzai *et al* /International Journal of ChemTech Research, 2018,11(08): 115-133.

DOI= <http://dx.doi.org/10.20902/IJCTR.2018.110813>

magnesium hydrogen phosphate (SrCrMHP) crystals by silica gel method and extended their research work and reported the growth of SrCaMHP crystals. Inorganic phosphates encompass a large class of diverse materials with numerous important industrial uses, e.g as catalysts, ion – exchange materials, solid electrolytes for batteries, in linear and non-linear optical components. The growth of these crystals depends upon the pH of the inner reactant and ionic concentration. Growth and characterization of calcium hydrogen phosphate dehydrate crystals was carried out by Madhurambal et al. [6]. Calcium hydrogen phosphate dehydrate (CHPD) is found quite frequently in urinary calculi (stones). The CHPD crystals were grown by the single diffusion gel growth technique in sodium metasilicate gel. Various kinetic and thermodynamic parameters for dehydration were estimated [7]. Several researchers have used gel technique to grow crystals and also modified them by suitable substitution to determine the effect of modification on their substitution. The impact of doping on crystalline quality of ammonium dihydrogen phosphate (ADP) has been studied by Gits et al [8]. To work on neodymium strontium phosphate was indeed motivated by the interesting range of applications known for these materials. The prime focus on neodymium doped strontium phosphate is because it has an effective and dominant hold on opto-electronic properties of material. Phosphates containing neodymium are found to be highly efficient laser crystals, good electrical and magnetic properties. Not only this, neodymium doped crystals have found a wide variety of application in military, industry, medical treatment and scientific research. So the emphasis was given on the growth of neodymium doped strontium phosphates because of their various merits in research purposes. To the best of author's knowledge, there is no such report of growth, structural and spectroscopic analysis of neodymium doped strontium phosphate crystals.

2. Experimental

2.1 Growth Mechanism

The growth of neodymium doped strontium phosphate (NdSrP) material was accomplished by controlled diffusion of Nd^{3+} and Sr^{2+} through silica gel impregnated with orthophosphoric acid. A mixture of strontium chloride (SrCl_2) and neodymium nitrate (NdNO_3) in the ratio of 1:1 by volume was gently poured along the sides of the tube over the perfectly set gel ensuring that this process does not break gel. The test tube was closed tightly to prevent evaporation. When the upper reactant ($\text{SrCl}_2 + \text{NdNO}_3$) came in contact with the lower reactant ($\text{H}_3\text{PO}_4 + \text{gel}$) the reaction started immediately. The slow diffusion of ions into the gel and their subsequent reaction with the phosphate ions resulted in the formation of expected materials. Light pink precipitates were formed instantly. The following reaction took place:



The purplish precipitation band increases in thickness gradually as the diffusion proceeds into the gel, resulting in the formation of narrow band below the precipitate which is visible in the formation of Leisegang ring. After 72 hrs, small nuclei appeared just below the precipitate formation. With time, the size of the nuclei increases and small spherulites were formed in the test tube as seen in Fig.1. The material was then taken out of the gel, washed thoroughly under running water and then dried. Fig.2 shows some of the synthesized NdSrP spherulites placed on the microslide. Table 1 gives the detail regarding various parameters used for growing neodymium doped strontium phosphate material. The various steps involved in the growth process are given in the following section.

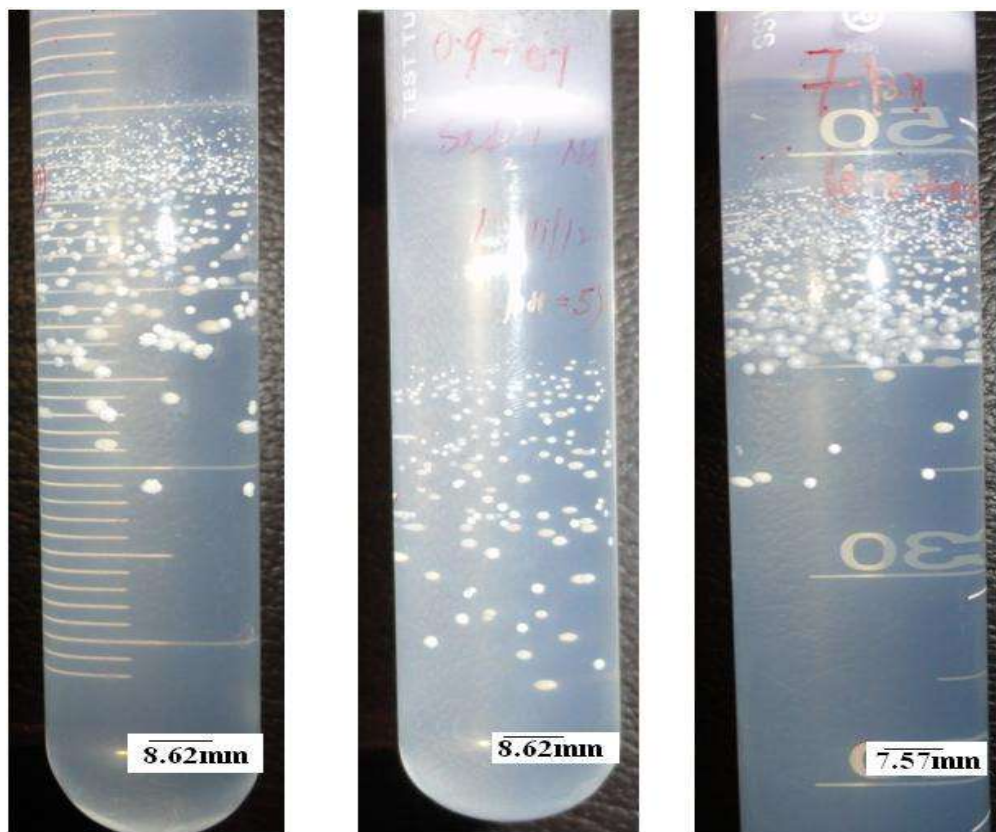


Fig. 1 Spherulites of neodymium doped strontium phosphate growing in crystallizer at pH 5, 6, 7 with different dopant concentrations.



Fig. 2 Spherulites of appreciable sizes grown at 10% doping concentration with pH value 5.

Table 1 Growth of spherulites and Liesegang ring formation at different pH for NdSrP

Gel + H ₃ PO ₄ (pH) value	Gel setting time in (h)	Supernatant concentration			Nucleation observed in (h)	Appearance of Liesegang's ring in (h)	Growth observed inside the growth medium
		Molarity	SrCl ₂	NdNO ₃			
5	72	0.5M	0.4	0.1	96	-	Spherulites,
6	48		0.4	0.1	48	72	
7	24		0.4	0.1	24	48	
5	120	1M	0.9	0.1	48	48	
5	120		0.8	0.2	48	-	

6	96	1M	0.9	0.1	24	-	White colored Granules with Liesegang rings are formed.
6	96		0.8	0.2	48	-	
7	24	1M	0.9	0.1	24	48	
7	24		0.8	0.2	24	48	

Preparation of Hydrosilica Gel

Hydrosilica gel was prepared by using the sodium metasilicate pentahydrate ($\text{Na}_2\text{SiO}_3 \cdot 5\text{H}_2\text{O}$) having 0.5 M concentration in 500 ml i.e., 53.035 g of sodium metasilicate (SMS) was dissolved in 500 ml of distilled water. This solution was then kept undisturbed for 1 day for sedimentation of insoluble particles and was kept airtight to keep it away from contact with the atmosphere, thereby, avoiding absorption of CO_2 . The solution was then filtered and stored, which was treated as stock solution. The pH of the SMS solution must be lowered in order to have proper gelation. This can be achieved by mixing an acid with solution. In the present case, orthophosphoric acid is used to adjust the pH of the solution. This orthophosphoric acid acts as the acidifying agent and also as the source of an anion needed for crystallization of compound.

Preparation of Lower Reactant

The lower reactant (H_3PO_4) was prepared by adding 12.6 ml of orthophosphoric acid in 450 ml of distilled water in order to have a solution of 0.5 molar concentrations. The solution was thoroughly mixed with the help of magnetic stirrer, kept undisturbed for 24 hours and then filtered. Phosphoric acid then was added drop by drop to SMS solution with continuous stirring with the help of magnetic stirrer to ensure the homogeneity of the medium. The pH of the resulting mixture was measured using digital meter immediately after proper mixing. In this way the solutions of desired pH value i.e. 4, 5, 6, 7 were obtained. The resulting mixture was then transferred into respective test tubes and kept undisturbed with their mouth covered for gelation.

Preparation of Upper Reactant

The upper reactant used consists of strontium chloride mixed with neodymium nitrate under different doping concentrations. For this purpose, 0.5 M of upper reactant was prepared by dissolving 1.75g of neodymium nitrate in 40 ml of distilled water and 4.26g of strontium chloride in 40 ml of distilled water to obtain two homogeneous solutions for 10% doping of neodymium in strontium phosphates. The two solutions were then mixed thoroughly using magnetic stirrer which gives the upper reactant. In the same way, the upper reactant of 1M concentration was prepared for 10% and 20% doping of neodymium in strontium phosphates.

2.2 Effect of Parameters

The various parameters which in one way or the other effect the growth of materials are the following.

- Effect of gel aging time with nuclei formed.
- Effect of concentration of upper reactant.
- Effect of dopant concentration.
- Effect of gel pH.
- Effect of surrounding temperature.

Effect of Gel Ageing Time with Nuclei formed

Gels were allowed to age for different periods before adding the feed solutions. It was found that as aging time of gel increased, the number of nuclei formed decreases as shown in Fig. 3. This is because gel ageing reduces the cell size and consequently the rate of diffusion of ions into the gel [1]. Gel ageing has pronounced effect on the size or the quality of the crystals. In the present work, gel aging has been done for 20 to 180 hrs for pH 5.

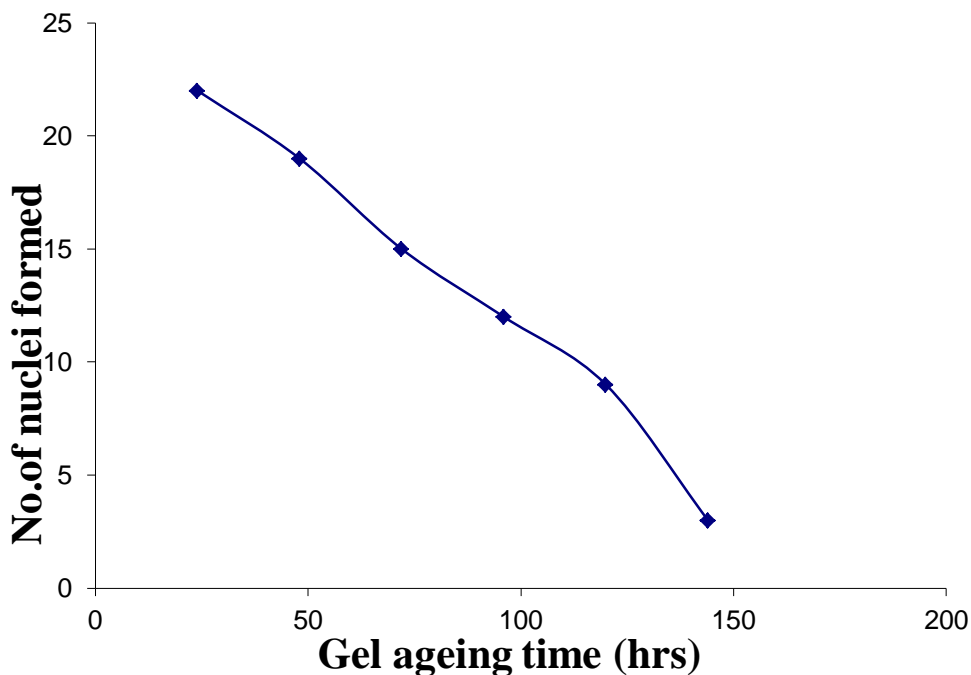


Fig. 3 Variation of number of nuclei formed with gel ageing time.

Effect of Concentration of Upper Reactant

A mixture of neodymium nitrate and strontium chloride is used as supernatant. Different concentrations of 0.5 M (10 %) and 1M (10%, 20%) were added over the set gel. It was observed that at 20% concentration less number of nuclei was formed and the growth rate was slow but at 10% supernatant concentration the nuclei formation was large in number and growth rate was steady as compared to the former one. The best growth was found at 0.5M (10%) concentration for pH 5 where the growth rate was fast and good junk of nuclei were formed whose proper growth led to formation of spherulites.

Effect of Dopant Concentration

The effect of neodymium doping on the growth of strontium phosphates was studied in a way that for 10% doping concentration larger number of nuclei were formed in comparison to 20% doping concentration. Although nucleation was observed at all doping concentrations yet the nucleation density was maximum at 10% doping concentration rather than for 20% doping concentration. Thus, 10% doping concentration at pH 5 was considered to be appropriate for further characterization analysis.

Effect of Gel pH

The effect of gel pH was considered in the present case by taking the pH values 4,5,6 and 7. When pH of gel was below 5 and above 7 no results were observed. So it was found that gel having pH between 5 and 7 gives best results and so the values less than 5 and greater than 7 are not conducive. As the pH of gel varies morphology of crystal varies which in one way or the other correlates with nucleation density. Nucleation density is minimum at pH 6 and maximum at pH 7. Fig. 4 shows the number of nuclei formed within a span of time at different pH.

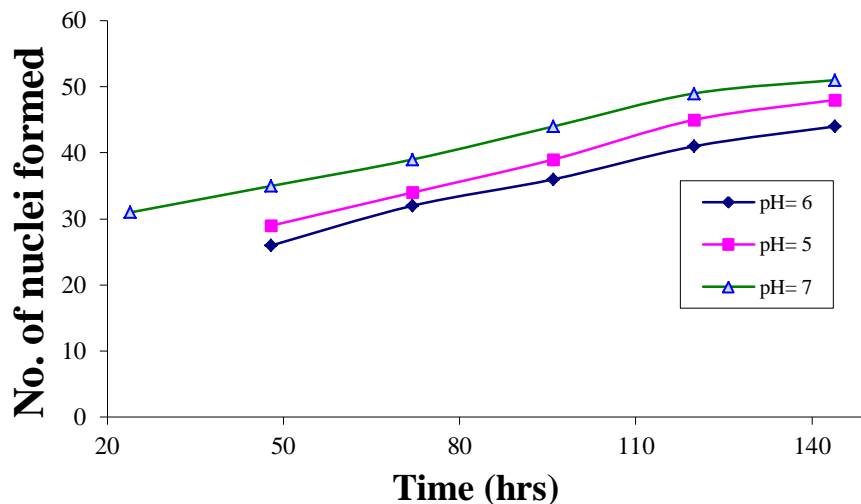


Fig. 4 Formation of number of nuclei with time at different pH values.

Effect of Surrounding Temperature

The effect of temperature on the nucleation and growth of many crystals has been studied by many people [9]. As the temperature increases, the free energy of formation of a critical nucleus increases but the degree of supersaturation decreases [10]. The surrounding temperature has a profound effect on the rate of reaction and diffusion. It was experimentally observed that temperature range of 30-40°C proved favorable for the growth of neodymium doped strontium phosphate crystals. The effect of various parameters on the preparation of the material was compiled and the optimum conditions are given in tabulation form in Table 2.

Table 2 Optimum conditions for the growth of NdSrP

Molarity of gel ($\text{Na}_2\text{SiO}_3 \cdot 9\text{H}_2\text{O}$)	0.5 M
Molarity of lower reactant (H_3PO_4)	0.5 M
Molarity of upper reactant ($\text{SrCl}_2 + \text{Nd}(\text{NO}_3)$)	0.5 M
Gelation period	72h
Gel pH	5
Temperature range	30-40°C

2.3 Characterization

The characterization techniques include powder X-ray diffraction (XRD), scanning electron microscopy (SEM), Fourier transform infrared spectroscopy (FTIR), ultraviolet-visible-near infrared (UV- VIS-NIR) absorption spectrophotometer. The phase identification was carried out by X-ray diffraction patterns using P Analytical X' Pert Pro diffractometer with a $\text{CuK}\alpha$ radiation ($\lambda=1.54060 \text{ \AA}$), the intensities of diffraction beam was obtained in 2θ range between 20° - 60° . Debye- Scherer relation and Williamson - Hall method was used to determine the crystallite size. The particle size was measured with a Zeta sizer Nano ZS (Malvern Instruments Ltd.; UK) analyzer. In order to study microstructures scanning electron microscope of JEOL model JSM-6390 LV was used. Fourier transform infrared (FTIR) spectrum was obtained on IR Prestige-21 (Schimadzu) spectrophotometer in the region from 400 - 4000 cm^{-1} . The measurements were made using KBr pellets containing 2 gm of powdered material. Spectral grade potassium bromide (KBR) was used for the preparation of pellets. The optical absorption was measured in UV-VIS- NIR region with Shimadzu UV 3600 spectrophotometer. The layer of powdered material is placed on the surface of reference material [barium sulfate (BaSO_4)] using a quartz crystal. The electrical characteristics which include behavior of dielectric constant with frequency and temperature were studied using automated impedance analyzer (LF 4192A model) interface with USB GPIB converter 82357 B (Agilent) and further automated by using a computer for data recording, storage and analysis.

3. Results and Discussion

3.1 Powder X-ray Diffraction

The powder X-ray diffraction (PXRD) method is considered to be the preliminary analysis in the characterization studies of the materials. Because of uniqueness of the X-ray diffraction pattern of each crystalline material, the X-ray provides a convenient and practical means for the quantitative identification of crystalline compounds. X-ray diffraction structure can be used to qualitatively determine the domain structure of polycrystalline material. The powder X-ray diffractogram of neodymium doped strontium phosphate hereafter abbreviated as NdSrP grown in silica gel is shown in Fig.5. The occurrence of highly resolved peaks at specific 2θ Bragg angles indicate the high crystallinity of the grown material. The crystal system in our case comes out to be triclinic with cell parameters- $a = 7.11\text{\AA}$, $b=6.71\text{\AA}$, $c=7.09\text{\AA}$, $\alpha=95.673^\circ$, $\beta= 103.8^\circ$, $\gamma=86.97^\circ$ and volume= 336.5\AA^3 . The XRD data was compared with standard values from JCPDS file number 33-1335. The interatomic spacing 'd' values of neodymium doped strontium phosphate were compared with the standard JCPDS files as shown in Table 3. The slight changes observed in the calculated interatomic spacing 'd' values may be due to presence of dopant (neodymium) into the host lattice of strontium phosphate. Thus, for neodymium doped strontium phosphate highly crystalline peaks are observed and the crystallite size was calculated using the Debye- Scherer (D.S) equation.

$$D=0.9\lambda/\beta \text{ Cos}\theta \quad (1)$$

where ' β ' represents full width at half maxima of X-ray diffraction lines, ' λ ' is the wavelength, ' θ ' is the Bragg's angle and ' K ' is a constant varying with crystal habit and chosen to be 0.9. The average crystallite size using Debye Scherer method is equal to 135 nm.

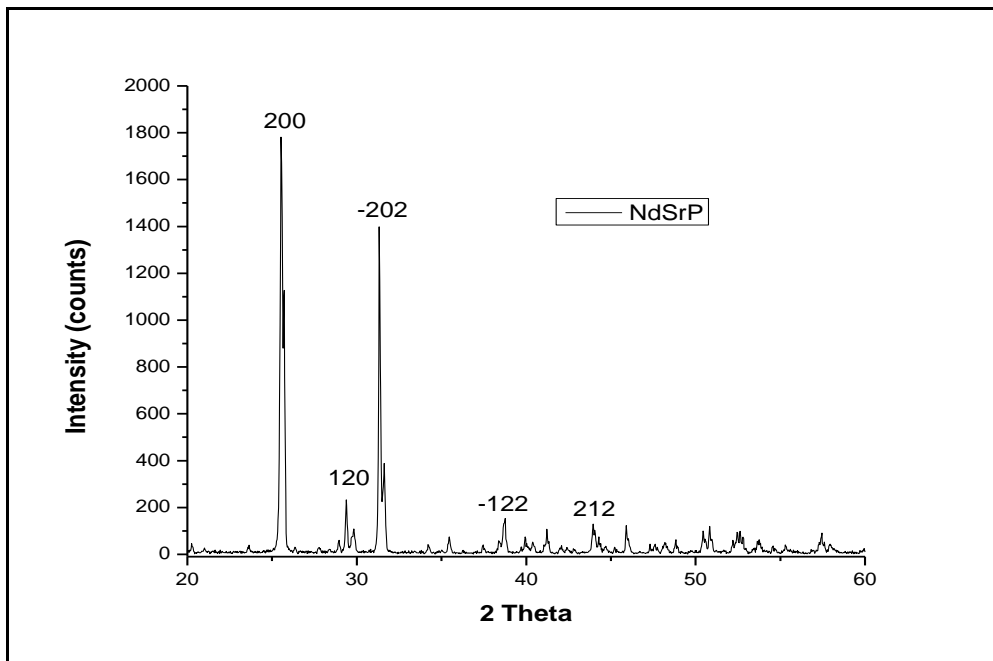


Fig. 5 Powder X-ray diffraction pattern of neodymium doped strontium phosphate indicating the formation of fine particles.

Table 3 Powder X-ray diffraction data of NdSrP

Angle 2θ	d \AA		h k l
	observed	calculated	
25.647	3.485	3.482	2 0 0
29.41	3.044	3.042	1 2 0
31.29	2.845	2.844	-2 0 2
38.53	2.534	2.531	-1 2 2
43.91	2.059	2.057	2 1 2

3.2 Scanning Electron Microscopy

The information regarding morphology and microstructure of neodymium doped strontium phosphate was investigated under scanning electron microscope (SEM) as shown in Fig.6. In order to study the surface features of grown material, scanning electron microscopy clearly observed that growth of neodymium doped strontium phosphate takes place in the form of fine nanoparticles and these particles have been further agglomerated in the form of elongated plates or envelopes. The average line intercept method was used to calculate the grain of the SEM micrograph of neodymium doped strontium phosphate whose value comes out to be 130 nm.

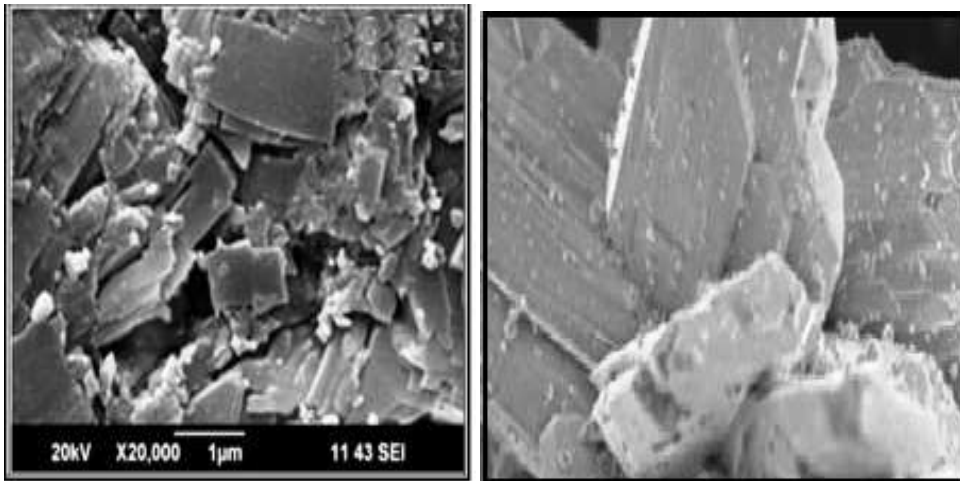


Fig. 6 Particle size analyzer of neodymium doped strontium phosphate.

In order to study the elemental composition of neodymium doped strontium phosphate (NdSrP), energy dispersive X-ray analysis (EDAX) was performed on the grown composition. Fig.7 depicts the EDAX spectrum of NdSrP that show peaks corresponding to all major elements present in the grown composition like neodymium, strontium, oxygen and phosphorous as should be expected in case for neodymium doped strontium phosphate. No such impurity was found in the grown material.

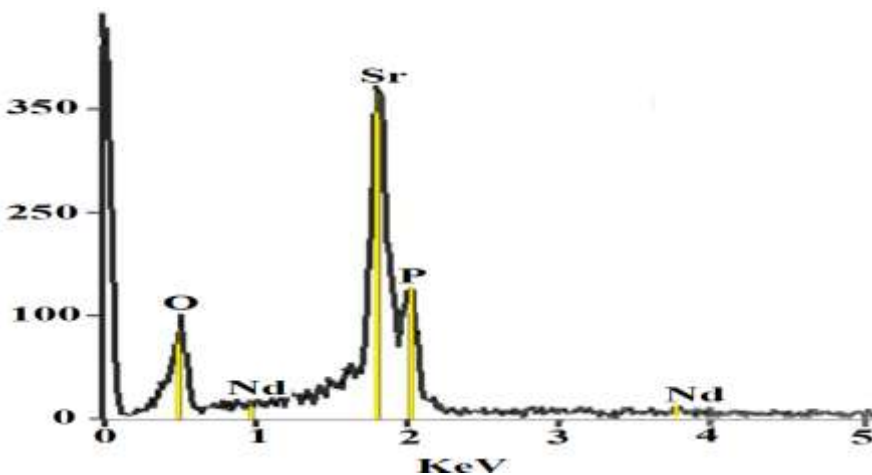


Fig. 7 Energy Dispersive X-ray analysis of NdSrPspherulites.

3.3 Particle Size Analyzer

The particle size measuring is a technique which belongs to the field of particle analysis. The graphs obtained from Zeta sizer (ZS) particle size (nm) analyzer showed relevant peaks indicating material belongs to the nano-range i.e., the fine range. Fig.8 shows relevant peak for neodymium doped strontium phosphate and

the particle size calculated from this method come out to be 140 nm. From the powder X-ray diffraction and SEM analysis we infer that the grown composition has been successfully prepared in the fine nanoscale region.

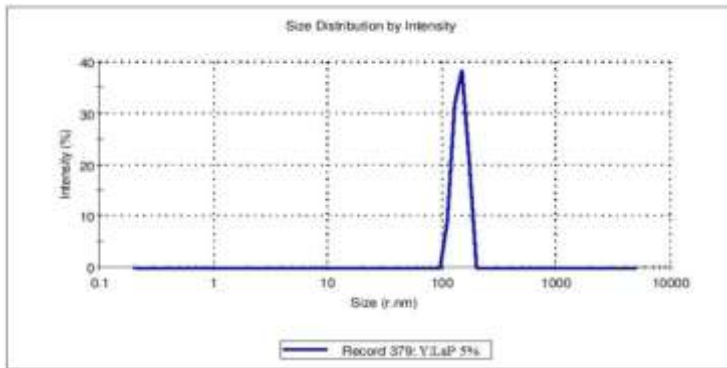


Fig. 8 Particle size analyzer of neodymium doped strontium phosphate.

3.4 Optical Absorption Analysis (Ultraviolet Spectroscopy)

The optical properties of materials provide an important tool for studying energy band structures, localized defects lattice vibrations etc [11]. The refractive index and band gap energy are two fundamental physical quantities that characterize a material's optical and electronic properties. Thus, the relevant applications of neodymium doped strontium phosphate (NdSrP) spherulites in optical and opto-electronic devices depend on knowing their characteristic values. In order to study the non linear optical applications, transmittance spectrum is a needed parameter. The transmission spectrum was recorded within the wavelength range 200 – 800 nm at room temperature as shown in Fig. 9. The optical transmittance range and transparency cut off are important in providing on the type of optical properties of crystal. On analyzing the graph, it is found that the lower cut off wavelength of the sample is 284 nm which authenticate the optical importance of these spherulites. The desired lower cut off wavelength in the transmittance analysis is to be between 200 and 300 nm for effective optical applications. Absence of absorption in region between 400 and 800 nm is an advantage as it is the key requirement for materials having non-linear optical properties.

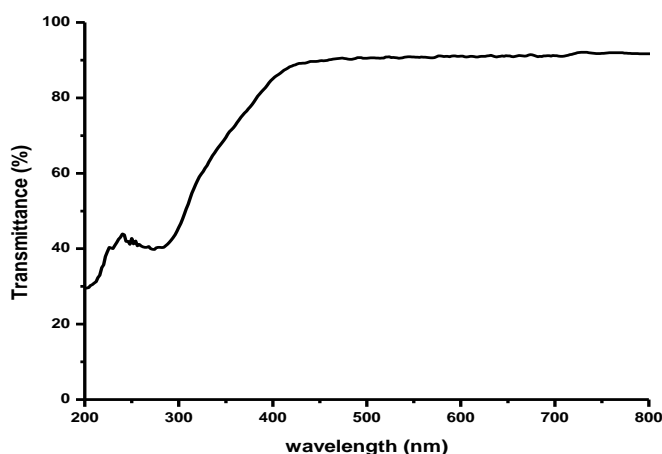


Fig. 9 UV-VIS transmission spectra of neodymium doped strontium phosphate.

Fig 10 shows the UV-VIS absorption spectra of neodymium doped strontium phosphate in the range 200-800 nm. The absorption of the sample lies in the ultraviolet range. The absorption peaks are seen at wavelengths 205 nm and 248 nm. The absorption of the neodymium doped strontium phosphate is very less, approximately equal to 0.6, thereby indicating that the sample is a good transmitter. Usually the transmittance of alkaline earth crystals lie in the range of 80-85%, but the transmittance of neodymium doped strontium phosphate is 89% [12]. This increase in the transmittance of the grown sample is due to the doping of neodymium in strontium phosphate.

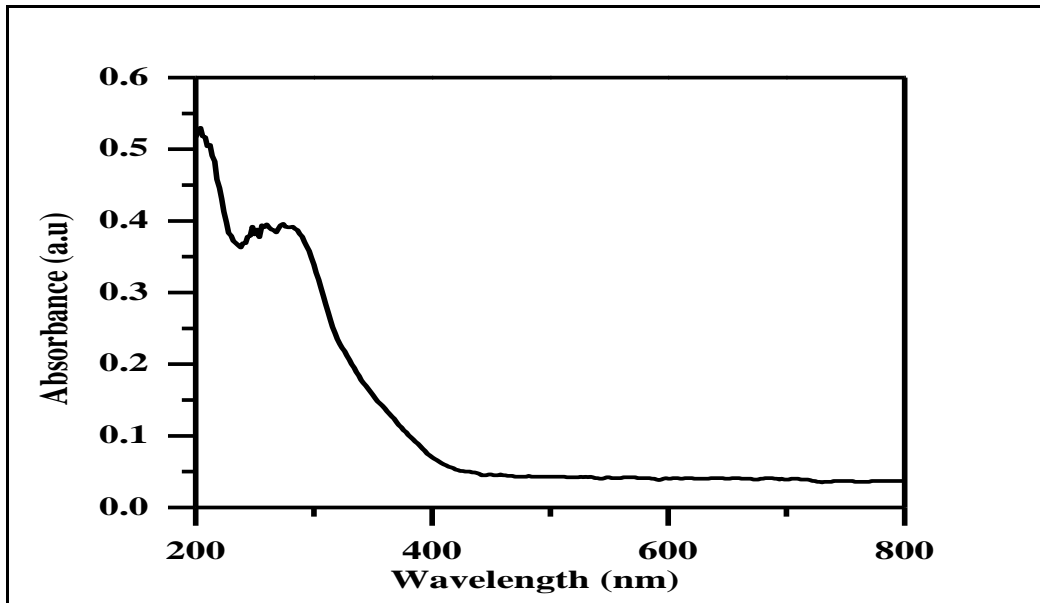


Fig. 10 UV-VIS absorption spectra of neodymium doped strontium phosphate.

The optical band gap energy can be determined from absorption spectrum using Tauc's relation[13]

$$\alpha h\nu = A (h\nu - E_g)^n \quad (2)$$

where 'A' is constant, 'hν' is the photon energy, 'E_g' is the optical band gap energy of the material and the exponent 'n' depends upon the type of transition. The energy band gap of the material can be obtained by plotting $(\alpha h\nu)^2$ versus hν and by extrapolating the linear portion of the absorption edge to find the intercept with energy axis. Tauc plot of neodymium doped strontium phosphate is shown in Fig 11. The optical band gap of neodymium doped strontium phosphate comes out to be equal to 3.7 eV. As a consequence of wide band gap, the grown material has high transmittance in the visible region, enhancing its optical quality and making it more suitable for optical applications.

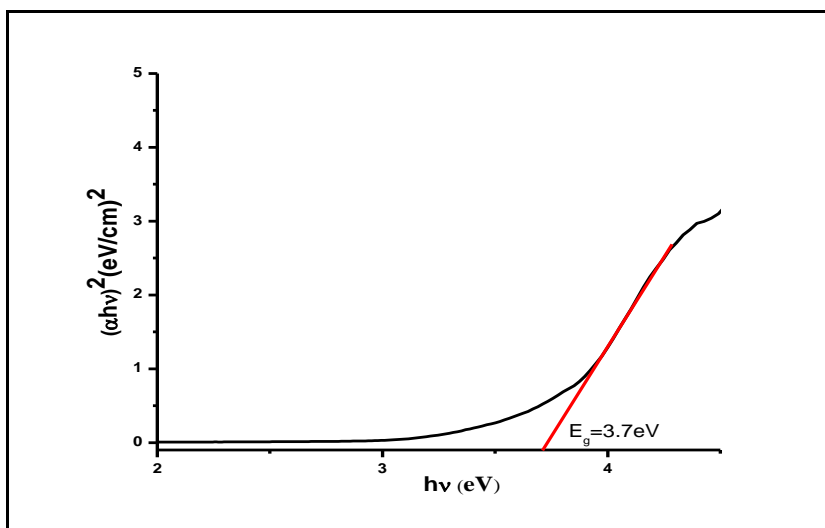


Fig. 11 Tauc plot showing band gap of neodymium doped strontium phosphate spherulites.

3.4.1 Determination of Optical Constants

The extinction coefficient indicates the amount of absorption loss when electromagnetic waves propagate through a material. Extinction coefficient (K) can be evaluated as follows:

$$K = \lambda\alpha/4\pi \quad (3)$$

where ' α ' is the absorption coefficient and ' λ ' is the wavelength of light. Extinction coefficient (K) can be evaluated for neodymium doped strontium phosphate spherulites as shown in Fig.12. Extinction coefficient (K) can be evaluated for neodymium doped strontium phosphate spherulites as shown in Fig. 12. The variation of extinction coefficient with photon energy clearly depicts that the extinction coefficient strongly depends upon photon energy. The extinction coefficient remains almost constant upto 2.9eV after which extinction coefficient shows a steep rise and then decrease again at 4.3 eV. NdSrPspherulites are exhibiting the extinction coefficient in powers of 10^{-6} which shows losses caused by absorbance and scattering processes are negligible that makes these materials more prominent for optical device application.

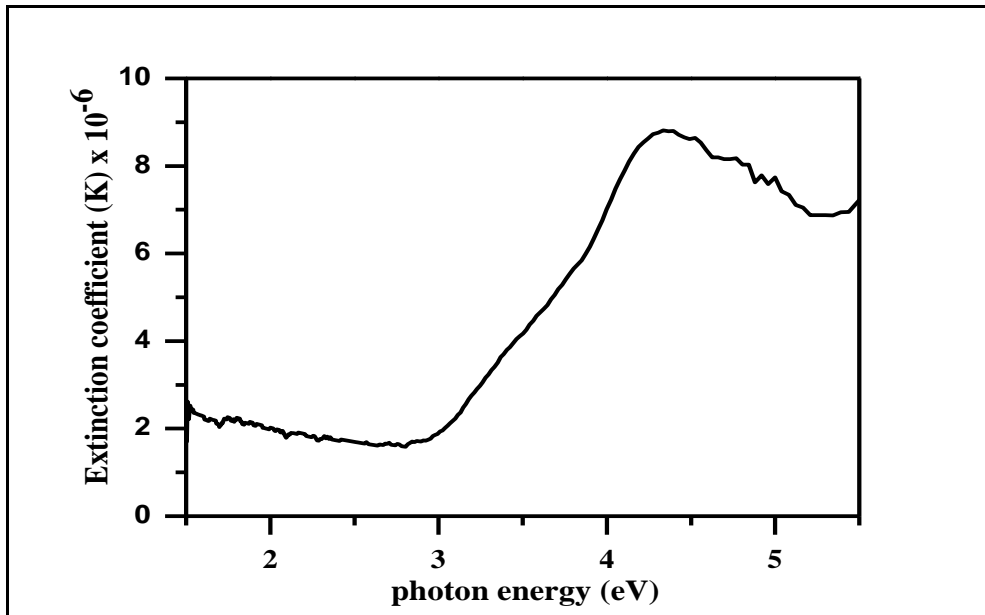


Fig. 12 Extinction coefficient versus photon energy of NdSrPspherulites.

The reflectance (R) in terms of the absorption coefficient can be calculated using the relation [14],

$$R = 1 \pm \frac{\sqrt{(1-\exp(-at)) + \exp(at)}}{1+\exp(-at)} \quad (4)$$

where ' α ' is the optical absorption coefficient, ' t ' is the thickness of the crystal.

The refractive index (n) was determined using reflectance data,

$$n = \frac{-(R+1) \pm \sqrt{3R^2 + 10R - 3}}{2(R-1)} \quad (5)$$

where ' n ' is the refractive index, ' R ' is the reflectance. Fig.13 shows the plot of refractive index as function of wavelength and it is clearly depicted that the refractive index decreases as the wavelength increases. The refractive index remains constant up to 300 nm and then it increases abruptly with further increase in the wavelength. Overall, the high transmittance and low refractive index values ($n = 0.4$) of NdSrPspherulites makes it useful for non-linear optical applications.

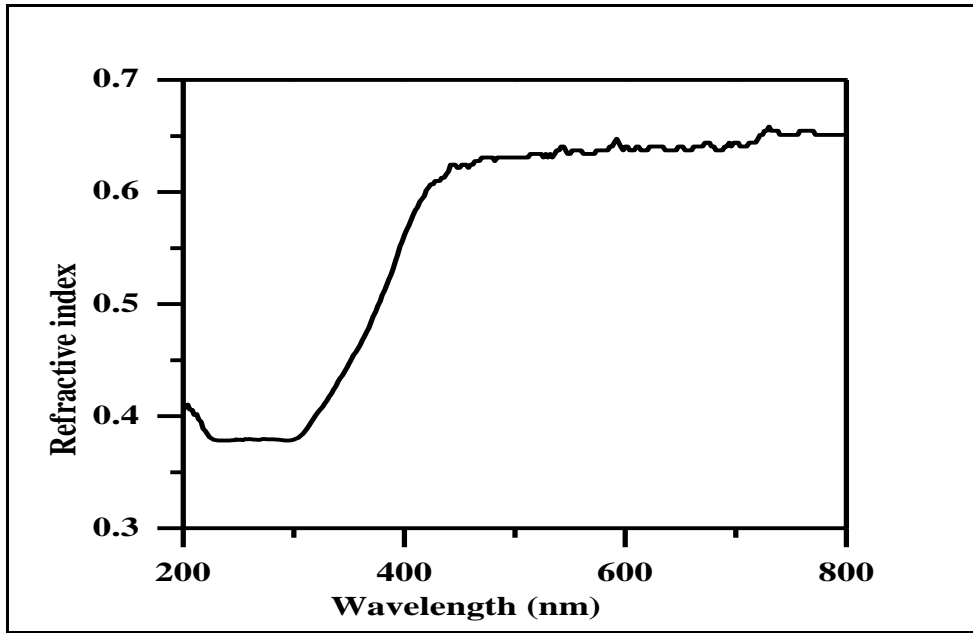


Fig. 13 Plot of refractive index with respect to wavelength for NdSrP.

The optical conductivity (σ_{op}), a measure of frequency response of the material when irradiated with light is related to refractive index ‘n’ and the speed of light ‘c’ as shown by the relation

$$\sigma_{op} = \frac{anc}{4\pi} \tag{6}$$

Also, the electrical conductivity(σ_e) is related to the optical conductivity as given by the relation

$$\sigma_e = \frac{2\lambda}{\alpha} \sigma_{op} \tag{7}$$

From Fig.14, it is clear that optical conductivity increases with increase in photon energy which confirms the presence of high photo response nature of material, whereas the electrical conductivity shows a decrease with increase in photon energy. Thus, the low extinction value and low electrical conductivity makes the material more dominant for device applications.

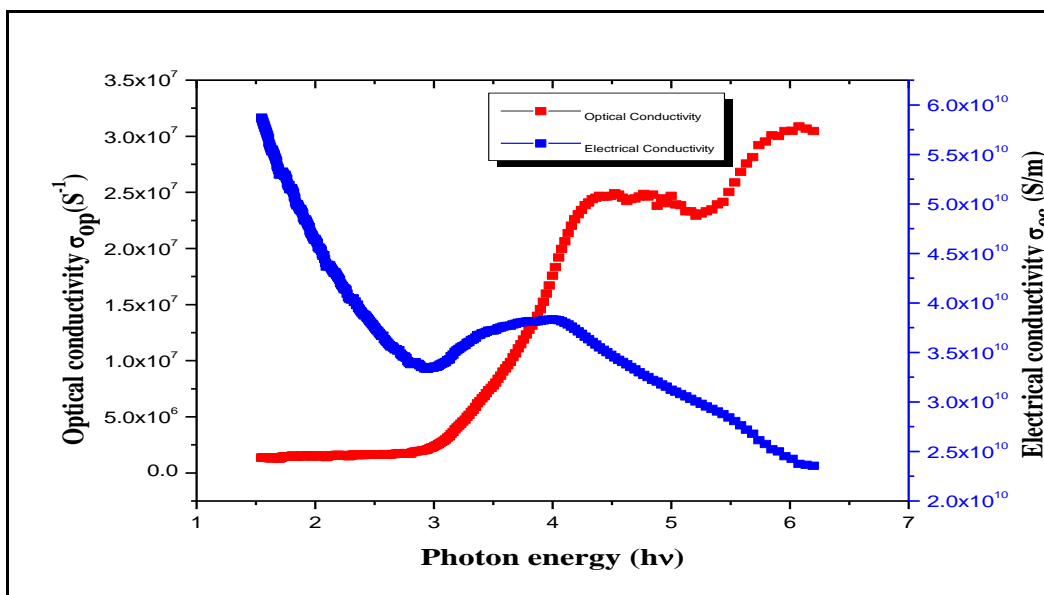


Fig. 14 Variation of optical conductivity and electrical conductivity with photon energy.

The electrical susceptibility (χ_c) is related to optical constants as given by relation [15]

$$\epsilon_r = \epsilon_0 + 4\pi\chi_c = n^2 - k^2 \quad (8)$$

$$\text{Hence } \chi_c = (n^2 - k^2 - \epsilon_0) / 4\pi \quad (9)$$

Where ' ϵ_0 ' is the dielectric constant in absence of any contribution from free carriers. The value of electrical susceptibility (χ_c) comes out to be 0.4825 as seen in Fig. 15.

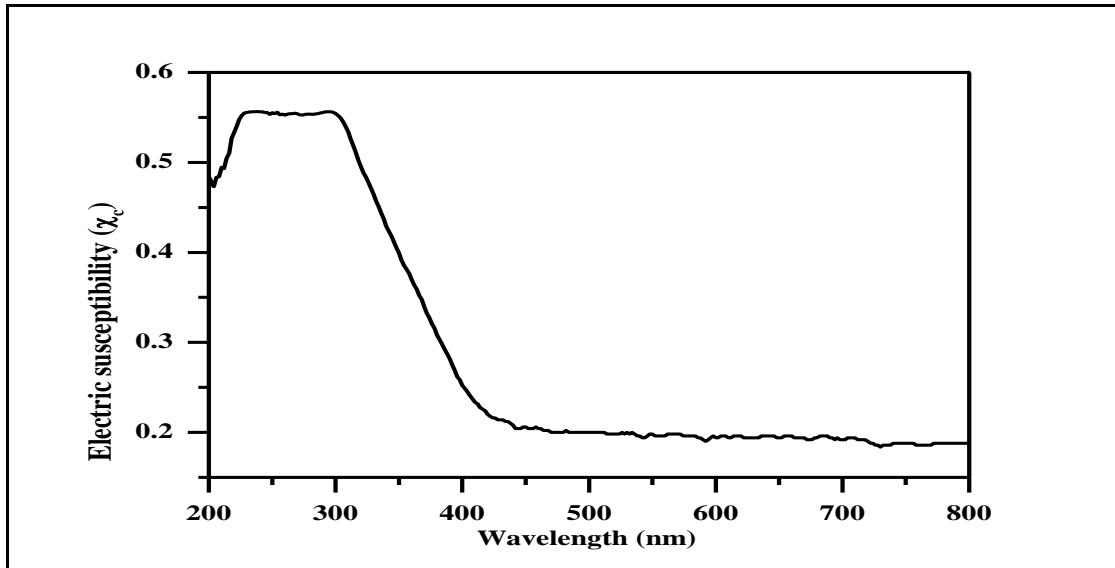


Fig. 15 Plot of electrical susceptibility with respect to wavelength of NdSrP.

The real part dielectric constant and imaginary part dielectric constant ' ϵ_r ' and imaginary part dielectric constant ' ϵ_i ' can be calculated following the relation [16]

$$\epsilon^* = \epsilon_r - \epsilon_i \quad \text{where } \epsilon_r = n^2 - k^2 \text{ and } \epsilon_i = 2nk \quad (10)$$

The value of real and imaginary dielectric constant at $\lambda = 800$ comes out to be 0.67 and 4.1×10^{-3} respectively. The lower value of the dielectric constant with a wide band gap of NdSrP spherulites suggests its suitability for optoelectronic devices [17].

3.5 Fourier Transform Infrared (FTIR) Spectroscopy

Fourier transform infrared (FTIR) spectrum is formed as a consequence of the absorption of electromagnetic radiation at frequencies that correlate with the vibration of specific sets of chemical bonds from a molecule. Fourier transform infrared (FTIR) spectrophotometer is an analytic instrument for detecting functional groups and rendering information regarding the bonds between the molecules. The major significance required for identification of the source of an absorption band is intensity (weak, medium or strong), shape (broad or sharp) and position in the spectrum. The FTIR spectrum shows the specific identification of O-H as well as P-O bonding as seen in Fig. 16. These peaks were identified in comparison with the earlier report [18, 19]. The stretching vibrations of HPO_4^{2-} ions show bands at 2448.92 and 2797.87 cm^{-1} . The band at 1737.68 cm^{-1} corresponds to hydroxyl group. The P = O stretching is depicted by bands at 1260.07 and 1081.51 cm^{-1} . The P - O asymmetric stretching is shown by bands at 995.31 and 884.30 cm^{-1} . The band at 569.99 cm^{-1} represents the P - P stretching along with the band at 425.65 represents the O - P - O bending mode as given in Table 4. When neodymium doped strontium phosphate spectrum was compared with the spectra of pure strontium phosphate, a shift in the peaks confirmed the incorporation of dopant ion into the host lattice. The force constant (F_c) for the symmetric and anti-symmetric stretching of P-O bond can also be calculated from the FTIR spectrum. The force constant (F_c) for P - O stretching calculated in case of NdSrP comes to be 4.18×10^5 dynes/cm whereas the force constant value for pure strontium phosphate is reported to be 4.98×10^5 dynes/cm. Thus, from the force

constant value one can conclude on addition of substitution (neodymium) into the host matrix of strontium phosphate there is decrease in the values of force constant.

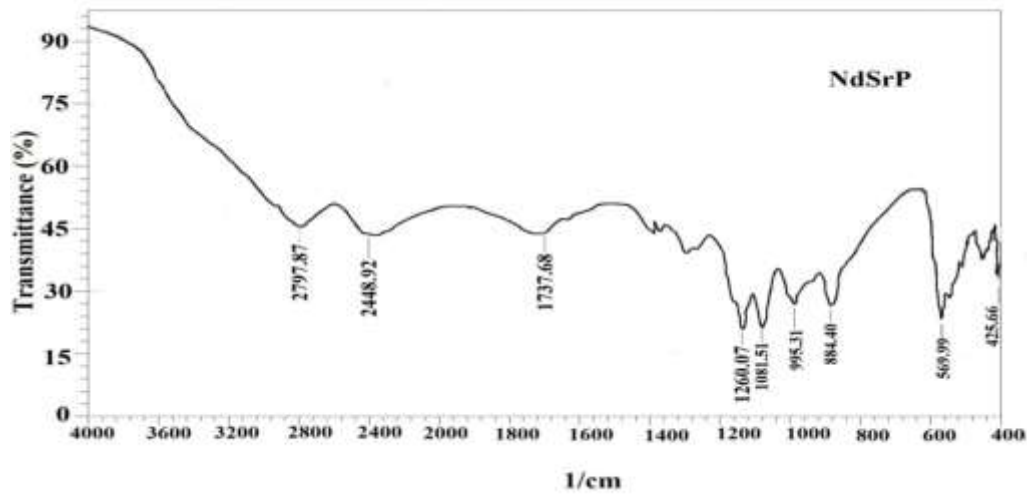


Fig. 16 Fourier transform infrared (FTIR) spectrum of NdSrP.

Table 4 Presence of various functional groups along with their frequency bands

S. No.	Assignments of band peaks	IR bands/cm NdSrP
1	Stretching vibrations of HPO_4^{2-} ion	2448.92-2797.87
2	OH	1737.68
3	P – O asymmetric stretching	995.31
4	P – P stretching	569.99
5	O-P-O bending	425.65

3.6 Dielectric Studies

The electrical property of this material was understood by finding the dielectric constant and studying its behavior at different frequencies and temperature. Dielectric characterization of a material indicates its response to an applied electric field. There are several reports regarding dielectric studies of single crystals, ceramics, glasses and polycrystalline materials [20-25]. A study of the variation in dielectric constant with temperature and frequency of the applied electric field is very useful in the study of phase transitions taking place in materials. In the present investigation dielectric constant and dielectric loss was studied and analyzed for different temperatures at different frequencies. The results obtained are given in the following sections.

3.6.1 Variation of dielectric constant with temperature at different frequencies

The dependence of dielectric constant on temperature was studied in the temperature range of 30-400°C and in the frequency range of 10 KHz to 1MHz of the applied a.c field and is shown in the Fig.17.

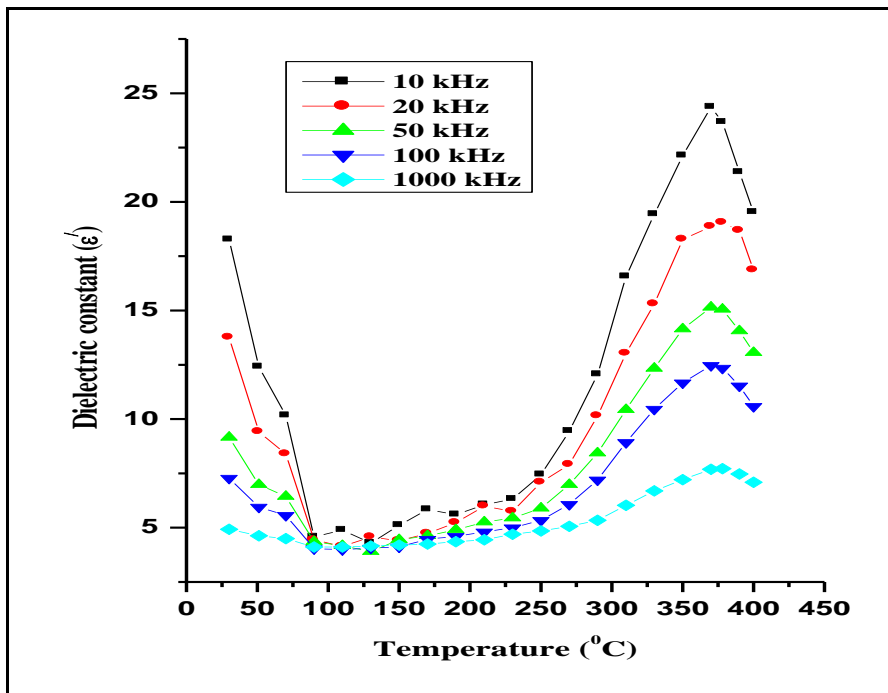


Fig. 17 Plot of dielectric constant versus temperature at different frequencies.

The behavior of dielectric constant with temperature for different frequencies can be divided into two regions. In the first region, the temperature range is 30-130°C, whereas for second region, the temperature ranges from 130-400°C.

Region I: 30-130°C

In this region, the dielectric constant shows a maximum value of ϵ' at each particular frequency which decreases as the temperature is increased from 30-130°C. The decrease in ϵ' value is less at frequency of 1000 kHz as compared to frequency of 10 kHz. The value of ϵ' at 30°C corresponding to the frequency of 10, 20, 50, 100 and 1000 kHz comes out to be 18.3, 13.7, 9.2, 7.2, 4.9 respectively whereas at 130°C, the values comes out to be 4.2, 4.5, 3.8, 4.0, 4.1 respectively. The analysis of data suggests that neodymium doped strontium phosphate has some values of dielectric constant below the room temperature (30°C). However, because of limitation of the instrument we are not able to find value of ϵ' below the room temperature. Therefore, from the behavior i.e., decrease in the value of ϵ' with increase in temperature suggests that there is some type of transition taking place in material below room temperature.

Region II: 130 – 400°C

In the temperature range of 130-250°C, there is no substantial change in the values of ϵ' for all the frequencies concerned. After 250°C, the ϵ' value increases substantially e.g. at a frequency of 10 kHz, the ϵ' value increases from 7.44 upto 24.36 at temperature of 370°C. Beyond this temperature, the value decreases and the same behavior is observed for other frequencies as well. Therefore, the peak value of dielectric constant in case of neodymium doped strontium phosphate is found to be 370°C for all the frequencies thereby, suggesting the ferroelectric transition temperature to be 370°C.

3.6.2 Variation of dielectric constant with frequency at different temperatures

The dependence of dielectric constant on frequency of applied a.c field for different temperature range 30-400°C is shown in Fig 18.

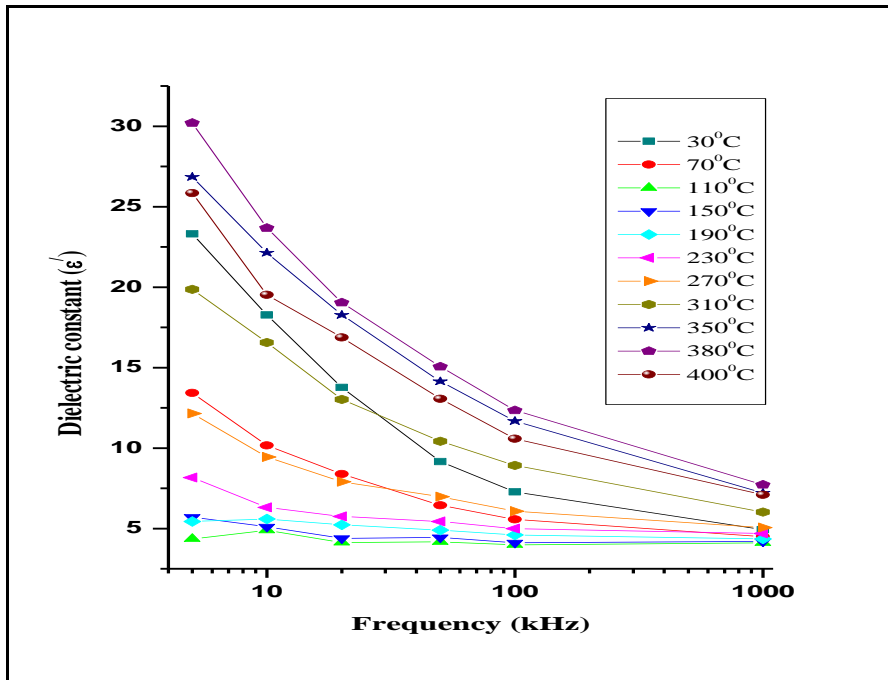


Fig. 18 Plot of dielectric constant versus frequency at different temperatures.

At each particular temperature, the dielectric constant shows decrease in its value as the frequency increases. This decrease in the value of ϵ' with increase in the frequency is the normal behavior and can be explained on the basis of polarization mechanism [26,28].

3.6.3 Dielectric loss and a.c conductivity

In the present case, the dielectric loss has been observed in the temperature range of 330°C-400°C. Fig. 19 shows the variation of $\tan(\delta)$ with temperature for different frequencies. From the figure, it is clear that dielectric loss increases with increase in temperature expect for the frequency of 1 MHz.

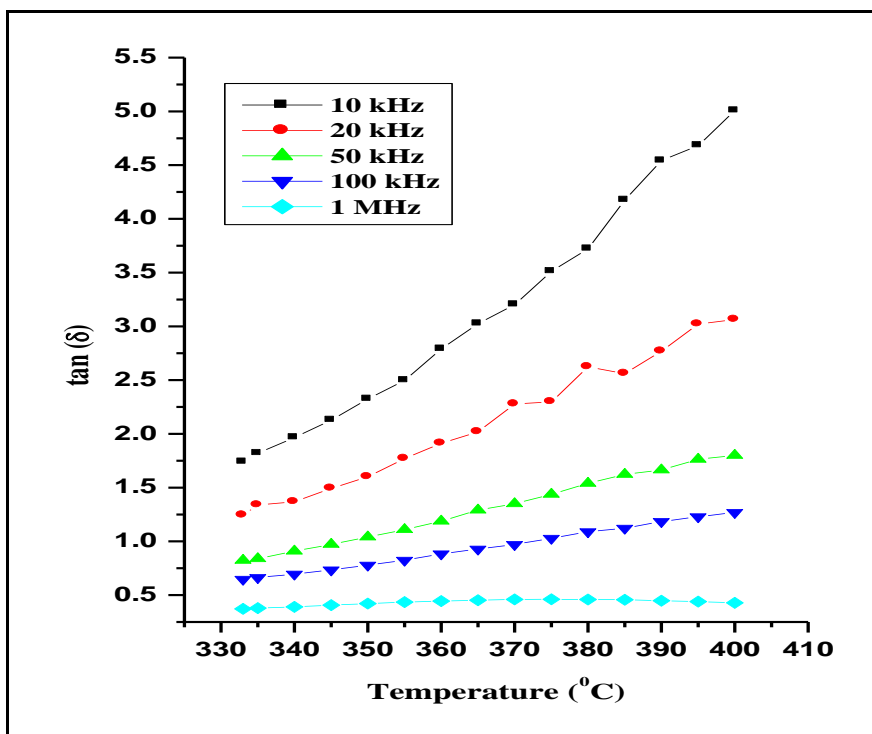


Fig. 19 Plot of dielectric loss $\tan(\delta)$ versus temperature at different frequencies.

From the dielectric loss, a.c conductivity was calculated using the relation:

$$\sigma_{ac} = 2\pi f_{ac} \epsilon_0 \epsilon' \tan \delta \quad (11)$$

Where f_{ac} is the frequency of the applied field (Hz), ϵ_0 is the absolute permittivity in free space having a value of $8.854 \times 10^{-12} \text{ Fm}^{-1}$, $\tan(\delta)$ is the dielectric loss. From the conductivity behavior, one can also understand and authenticate the conduction mechanism for neodymium doped strontium phosphate in high temperature region. The plot a.c conductivity ($\ln \sigma_{ac}$) as a function of temperatures for frequencies 5, 10, 20 and 50 kHz reveals that a.c conductivity increases with increase in temperature which is characteristic feature of materials where hopping mechanism dominates. The variation of $\ln \sigma_{ac}$ with $1000/T$ is shown in Fig 20. With the help of this curve one can evaluate the activation energy using the Arrhenius formulae: $\sigma_{ac} = \sigma_0 \exp(-E_a/K_B T)$, where ' σ_{ac} ' is the conductivity at temperature T, E_a is the activation energy for the electrical process and K_B is the Boltzman constant. Activation energy calculated from the slope of the graph using linear fit mechanism comes out to be 0.21, 0.19, 0.17, 0.15eV at frequencies of 5, 10, 20 and 50 KHz respectively. From the values of activation energy, it is clear that as frequency increases, the value of activation energy decreases and this type of behavior suggests that the conduction mechanism may be due to hopping of charge carriers i.e., (n or p type) from one site to another. Therefore, a very small of energy is required to activate the charge carriers/electrons for electrical conduction.

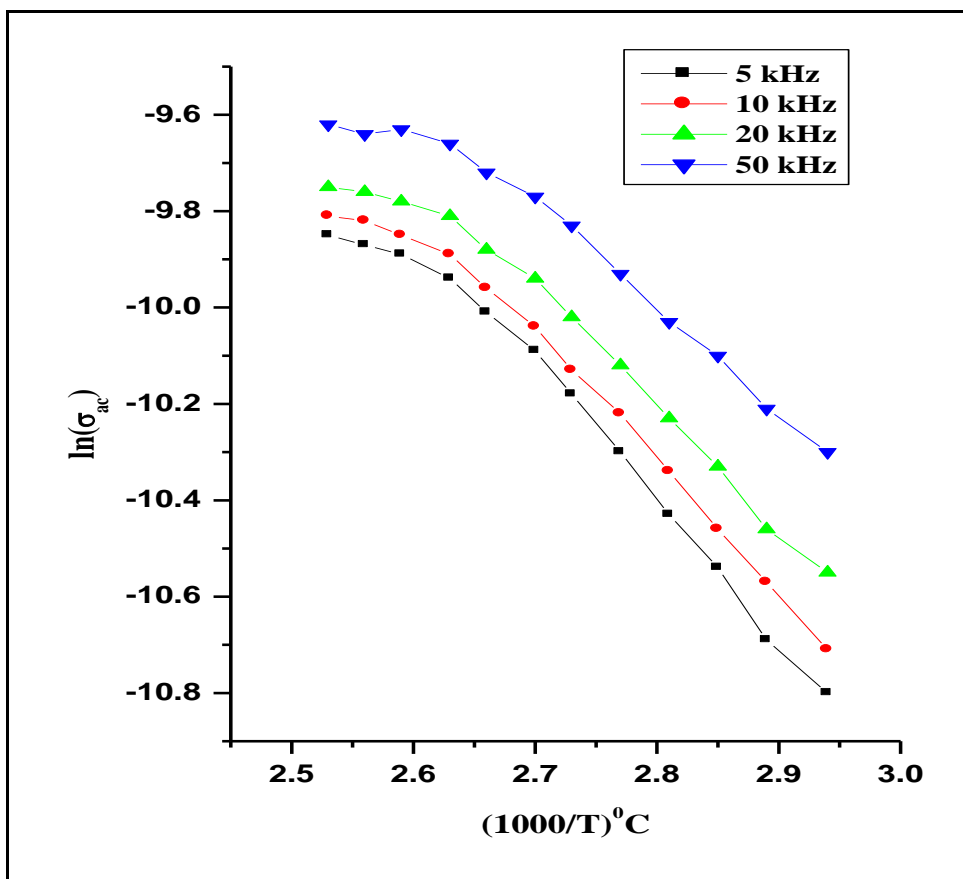


Fig. 20 Plot of $\ln \sigma_{ac}$ versus $(1000/T)^\circ \text{C}$ for different frequencies

4. Conclusions

From the analysis being done on neodymium doped strontium phosphate, one can draw that neodymium doped strontium phosphate can be synthesized successfully by room temperature solution technique i.e., gel technique and shows good optical and electrical properties. The powder X-ray diffraction results reveal that the grown material have triclinic crystal system. The particle size analyzer confirms the average crystallite size lies in the fine range that comes out to be 140 nm. UV absorption spectroscopy shows good optical transmittance in the visible and IR range. The UV cut off wavelength is found to be 284 nm. The low absorption in visible region suggests its susceptibility for non-linear optical properties. Fourier transform

infrared spectroscopy confirms the presence of relevant bands for neodymium doped strontium phosphate spherulites. The dielectric constant shows a peak at 370°C for all values of frequency ranging from 10 kHz to 1MHz. The transition temperature obtained in case of neodymium doped strontium phosphate (NdSrP) is 370°C. The activation energy calculated at frequencies 5, 10, 20 and 50 kHz comes out to be 0.21, 0.19, 0.17 and 0.15 eV respectively. The value of activation energy decreases with increase in frequency suggesting that the conduction mechanism is due to hopping of the charge carriers from one site to another. Therefore, a very small amount of energy is required to activate the charge carriers for electrical conduction.

References

1. Henisch H. K., Crystal growth in gels, Dover Publications Inc. New York 1996.
2. Blank Z., Speyer D. M., Brenner W., Okamoto Y., Growth of single crystals of silver halides in silica gels at near ambient temperatures, *Nature*, 1967, 216, 1103.
3. Barta C., Zemlicka J., Growth of CaCO₃ and CaSO₄ · 2H₂O crystals in gels, *J. Cryst. Growth*, 1971, 10, 158.
4. Koelmans H., Cox A.P.M., Luminescence of modified tin-activated strontium orthophosphate, *J. Electrochem. Soc.*, 1957, 104, 442.
5. Kanchana G., Suresh P., Sundaramoorthi P., Kolainathan S., Jeyanthi G. P., Growth of strontium chromium magnesium hydrogen phosphate (SrCrMHP) crystal in silica gel medium at different growth environments and nucleation reduction strategy, *J. of Min. and Mat. Charact. and Eng.*, 2008, 7 (3), 215.
6. Madhurambal G., Subha R., Mojumda rS. C., Crystallization and thermal characterization of calcium hydrogen phosphate dihydrate crystals, *J. of Therm. Anal. Cal.*, 2009, 96, 73.
7. Joshi V. S., Joshi M. J., FTIR spectroscopic, thermal and growth morphological studies of calcium hydrogen phosphate dihydrate crystals, *Crys. Res. Tec.*, 2003, 38 (9), 817-821.
8. Gits S., Robert M. C., Lefauchaux L., Doping effect on the crystalline quality of ADP doped with chromium: I. Comparison of solution-grown and gel-grown crystals, *J. Cryst. Growth*, 1985, 71, 203.
9. Patel A. R., Venkatesware Rao A., Gel growth and perfection of orthorhombic potassium perchlorate single crystals, *J. Cryst. Growth*, 1979, 47, 213.
10. Arimington A. F., O'Connor J. I., The gel growth of clear cuprous chloride crystals, *Mater. Res. Bull.*, 1967, 2, 907.
11. Dalal J., Kumar B., Bulk crystal growth, optical, mechanical and ferroelectric properties of new semiorganic nonlinear optical and piezoelectric lithium nitrate monohydrate oxalate single crystal, *Optical Materials*, 2016, 51, 139.
12. Praveena G.L., Balu T., Sreedevi R., Growth and characterization of BIS L-alanine strontium nitrate single crystals, *Journal of Applied Physics*, 2016, 8, 61.
13. Tauc J., Amorphous and liquid semiconductors, J. Tauc Edition Plenum, New York, 1974.
14. John J., Christuraj P., Anitha K., Bala Subramanian T., Band gap enhancement on metal chelation: Growth and characterization of cobalt chelated glycine single crystals for optoelectronic applications, *Mat. Chem. and Phy.*, 2009, 118, 284.
15. Dhanaraj P.V., Sudan T., Rajesh N.P., Synthesis, crystal growth and characterization of a semiorganic material: calcium dibromide bis(Glycine) tetrahydrate, *Curr. Appl. Phy.*, 2010, 10, 1349.
16. Dalal J., Kumar B., Bulk crystal growth, optical, mechanical and ferroelectric properties of new semiorganic nonlinear optical and piezoelectric Lithium nitrate monohydrate oxalate single crystal, *Opt. matr.*, 2016, 51, 139.
17. Besky Job C., Growth, structural, optical, thermal and photo conductivity studies of Potassium HeptaFluoroAntimonate crystals, *Arch. of Appl. Sci. Res.*, 2015, 7, 118.
18. Nakamoto K., IR and Raman Spectra of Inorganic compounds, 4th edition Wiley & Sons, New York 1986.
19. Cross A. D., Jones R., An introduction to Practical Infrared Spectroscopy, 3rd edition 1968.
20. Pandita S., Tickoo R., Bamzai K. K., Kotru P.N., Dielectric characteristics of gel grown mixed rare earth (Didymium) heptamolybdate crystals. *Mater Sci&Eng B.*, 2001, 87, 122.
21. Kumar A. V. R., Apparao B., Veeraiah N., Dielectric properties of LiF-B₂O₃-glasses doped with certain rare earth ions, *Bull. Mater. Sci.*, 1998, 21 (4), 341.
22. Prasad N. V., Prasad G. V., Bhimasankaram T., Kumar Suryanarayana G. S., Synthesis, impedance and dielectric properties of LaBi₅Fe₂Ti₃O₁₈, *Bull. Mater. Sci.*, 2001, 24 (5), 487.

23. Lingwal V., Semwal B. S., Panwar N. S., Dielectric properties of $\text{Na}_{1-x}\text{K}_x\text{NbO}_3$ in orthorhombic phase, Bull. Mater. Sci., 2003, 26 (6), 619.
24. Kang B. S., Choi S.K., Diffuse dielectric anomaly in MnO_2 -doped $\text{Pb}_{0.9}\text{La}_{0.1}\text{TiO}_3$ ceramic in the temperature range of 400–700 °C, J. Mater. Res., 2002, 17 (1), 127.
25. Srinivas K., Sarah P., Suryanarayana S.V., Impedance spectroscopy study of polycrystalline $\text{Bi}_6\text{Fe}_2\text{Ti}_3\text{O}_{18}$, Bull. Mater.Sci., 2003, 26 (2), 247.
26. Arora S.K., Patel V., Amin B., Kothari A., Dielectric behaviour of strontium tartrate single crystals, Bull. Mat. Sci, 2004, 27, 141.
27. Parekh B.B., Vyas P.M., Vasant S., Joshi M.J., Thermal, FT-IR and dielectric studies of gel grown sodium oxalate single crystals, Bull.Mat. Sci., 2008, 31, 143.
